Composites: Part A 43 (2012) 1120–1133

Contents lists available at SciVerse ScienceDirect

Composites: Part A

journal homepage: www.elsevier.com/locate/compositesa

Properties of thermo-chemically surface treated carbon fibers and of their epoxy and vinyl ester composites

F. Vautard [a,*], S. Ozcan [a], H. Meyer [b]

[a] Polymer Matrix Composites Group, Materials Science and Technology Division, Oak Ridge National Laboratory, Oak Ridge, TN 37831, USA
[b] Microscopy Group, High Temperature Materials Laboratory, Materials Science and Technology Division, Oak Ridge National Laboratory, Oak Ridge, TN 37831, USA

ARTICLE INFO

Article history:
Received 7 October 2011
Received in revised form 20 February 2012
Accepted 25 February 2012
Available online 4 March 2012

Keywords:
A. Carbon fiber
A. Polymer–Matrix Composites (PMCs)
B. Fiber/matrix bond
B. Surface properties

ABSTRACT

Carbon fibers were surface treated by a continuous gas phase thermo-chemical treatment. The surface and the mechanical properties of the fibers were investigated before and after treatment and compared to the properties obtained with a conventional industrial electro-chemical surface treatment. The increase of the oxygen atomic content was much sharper, the surface chemistry was better controlled, and the tensile strength of the fibers increased slightly with the thermo-chemical surface treatment. The thermo-chemical surface treatment created a topography which amplitudes were under 10 nm, thus creating some mechanical interlocking with the matrix. The electro-chemical surface treatment did not generate such a topography. The improvement of interfacial adhesion with a vinyl ester matrix was limited, revealing that oxidation of the carbon fiber surface alone cannot tremendously improve the mechanical properties of carbon fiber–vinyl ester composites.

© 2012 Elsevier Ltd. All rights reserved.

1. Introduction

The physico-chemical and mechanical properties of a composite material are not only depending on the characteristics of the reinforcement material and the matrix but also on the properties of the interface, which depend on the conditions used during the manufacturing [1]. Aside from the type of fiber, factors that influence interfacial adhesion in carbon fiber reinforced composites are mechanical interlocking [2], physical interactions (dispersive [3], polar [4], acid–base [5]) and chemical interactions [6], the presence of defects [7], and remaining stress due to the thermal treatment [8] or the shrinkage of the matrix [9]. It was also demonstrated [10] that surface treatments of carbon fiber act in two ways: some weak boundary layers generated during the carbonization of the precursor are removed and the surface properties are modified in order to monitor one or several of the parameters previously cited. Each type of matrix requires a specific fiber surface treatment in order to achieve an adequate interfacial adhesion. Some surface treatments can improve interfacial adhesion with a certain type of resin and lead to a weak interfacial adhesion with another type of resin [11,12]. Electrochemical surface treatments are still widely used, especially for the industrial production of carbon fibers. That is why an impressive number of electrolytes have been tested. Among them are phosphoric acid [13], sulfuric acid [14], nitric acid [15], alkaline solutions [16], ammonium salts [17], bleach [18], and potassium nitrate [19]. The fibers are washed in water after electro-oxidation in order to remove the excess of electrolyte, to avoid a typical contamination with ions like Na^+, Ca^{2+}, Cl^- [20,21] and to remove the carbon products detached from the surface of the fiber. A drying step follows before further processing, but a significant amount of water often remains on the surface [22]. Some effort is needed in order to provide a more environmentally friendly and energy effective surface treatment technology with no disposal of liquid waste. Moreover, the oxygen content generated by electro-chemical surface treatments without significant damage of the mechanical properties is limited. Indeed, strong oxidations create pits in the structure of the fiber [23,24] that can affect its mechanical properties, so the atomic oxygen content measured by X-ray Photoelectron Spectroscopy (XPS) is usually comprised between 7% [25] and 15% [26]. An alternative to surface treatments in an aqueous phase is plasma oxidation surface treatments in different gases such as air [27], oxygen [28] and carbon dioxide [29]. The transfer of these technologies to an effective continuous process has not yet been reported in the literature. Treatments creating radicals in the surrounding atmosphere under radiation gave some interesting results in the case of γ radiation [30], electron [31] and ion beams [32], but their direct application for the mass production of carbon fibers seems to be compromised. An oxidation in ozone at high temperature appeared to be a surface treatment technology that had the potential to be scaled-up for industrial production. Indeed, Fu et al. [33] used a batch process in which pitch-based carbon fibers were exposed to ozone at 160 °C during 5 min, which led to an improvement of the

* Corresponding author. Tel.: +1 865 574 9059; fax: +1 865 574 8257.
E-mail address: vautardf@ornl.gov (F. Vautard).

1359-835X/$ - see front matter © 2012 Elsevier Ltd. All rights reserved.
http://dx.doi.org/10.1016/j.compositesa.2012.02.018

Table 1
Physical properties of Panex® 35 carbon fibers (manufacturer's data).

Tensile strength (MPa)	Tensile modulus (GPa)	Density (g/cc)	Diameter (μm)
4137	242	1.81	7.2

mechanical properties of carbon fiber-cement composites. Jin et al. [34] used a batch process to surface treat pitch-based carbon fibers at high temperature in a vacuum system, keeping the ozone pressure at 0.4 MPa. They improved the mechanical properties of carbon–carbon composites. In this study, the characterization of a continuous surface treatment based on a gas phase thermo-chemical approach which is ready to be implemented in the industry is presented. The surface properties and the tensile strength of the fibers treated with this technology are compared to the ones obtained via conventional and commercial electro-chemical surface treatment. The mechanical properties of corresponding epoxy and vinyl ester composites are also investigated.

2. Materials and methods

2.1. Surface treatment of the carbon fibers

PolyAcryloNitrile (PAN) based high strength carbon fibers Panex®35 (50 k), produced by Zoltek Co. were used in this study. The fibers were neither surface treated and nor sized. The physical properties of the fibers surface treated and sized by the manufacturer are presented in Table 1.

As received carbon fibers were continuously surface treated in a reactive gas phase containing ozone. Ozone was produced by a PWB-150g ozone generator from Plasma Techniques Inc. The residence time of the fibers in the reactive gas phase was 2 min.

Panex®35 carbon fibers surface treated with the manufacturer's electrochemical surface treatment were also studied in order to compare the surface properties obtained with different surface treatments.

2.2. Characterization of the fiber properties

For the observation of the fiber surface, a Jeol 6500 FE-SEM was used in secondary electron mode. The fibers were fixed on the sample holder with carbon tape and without any kind of conductive coating. The acceleration voltage was 5 kV and the intensity of the emission current was 60 μA. ImageJ software was used for image analysis.

A Veeco D3000 Atomic Force Microscope (AFM), controlled by the software Nanoscope III, was used in tapping mode to observe the features of the surface topography at a nanometric scale. Single fibers were deposited on a mica disk and secured at their end with adhesive tape. Images of 2 μm × 2 μm were obtained.

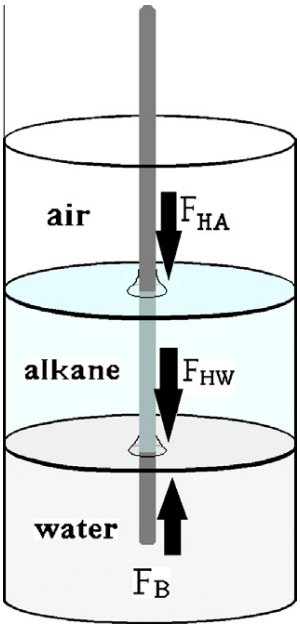

Fig. 1. The two liquid phase method with the use of an electrobalance. (For interpretation of the references to colour in this figure legend, the reader is referred to the web version of this article.)

X-ray Photoelectron Spectroscopy (XPS) analysis of the carbon fiber surface was carried out with a Thermo Scientific K-Alpha X-ray photoelectron spectrometer equipped with a conventional electron energy analyzer. The latter was operated in the Fixed Transmission Mode at constant pass energy of 200 eV for the survey spectra and 50 eV for the core level spectra. A monochromatic Al Kα source (1486.6 eV) operated at 420 W (14 kV; 30 mA) was used as incident radiation. Photo-emitted electrons were collected at a take-off angle of 90° from the sample and the pressure was about 10^{-9} mbar (10^{-7} Pa). The spectrometer energy scale was calibrated with respect to Ag 3d5/2, Au 4f7/2 and Cu 2p3/2 core level peaks, set with binding energies of 368.3, 84.0 and 932.7 eV respectively. All binding energies are referenced to the adventitious C(1s) peak located at 284.6 eV. Instrumental sensitivity factors were taken as C(1s):O(1s):N(1s) equals 1.000:2.930:1.800, respectively. C(1s), O(1s) and N(1s) core level spectra were fitted to GL function (product of a Lorentzian by a Gaussian) using Avantage 4.44 software. The background was a Tougaard type. The parameters controlling the shape of the asymmetric component (graphitic component) were determined with the C(1s) core level spectra of the untreated fiber because of its very low concentration of oxygen. The component peaks position used in C(1s), O(1s) and N(1s) curve fitting are presented in Table 2. There is evidence that

Table 2
Component peaks used in the fitting of C(1s), O(1s) and N(1s) peaks.

C(1s)		O(1s)		N(1s)	
Binding energy (eV)	Component peak	Binding energy (eV)	Component peak	Binding energy (eV)	Component peak
284.4 ≪ 284.6	Csp^2	531,2 ≪ 531,4	Ph=O (quinone), Ph—C=O,	398,4 ≪ 399,0	Pyridine
284,9 ≪ 285,1	Csp^3	532,0 ≪ 532,2	C=O (ester, anhydride, amide)	399,4 ≪ 399,8	Amines, amides, nitriles
284,8 ≪ 285,0	C—COOR	532,7 ≪ 532,9	R—OH, C—O—C	400,1 ≪ 400,7	Pyrrolidine, pyridone
285,4 ≪ 285,6	C—N	533,5 ≪ 533,7	Ph—OH, C—O (ester, anhydride)	401,1 ≪ 401,7	Pyridinium, protonated N
286,1 ≪ 286,4	C—O—R, C≡N	534,8 ≪ 535,2	Chemisorbed H_2O	405,5 ≪ 405,7	NO_x
287,4 ≪ 287,6	C=O	536,2 ≪ 536,6	Physisorbed H_2O		
288,3 ≪ 288,9	COOR	538.2 ≪ 538.6	Shake up		
290,1 ≪ 290,5	Physisorbed H_20				
291,3 ≪ 291,7	Shake up				

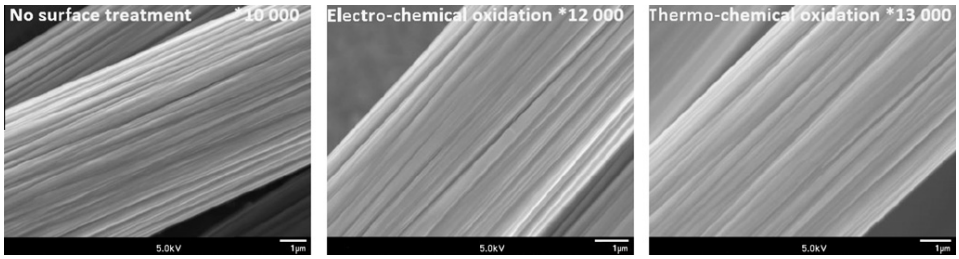

Fig. 2. SEM images of the surface of carbon fibers before and after oxidative surface treatments. (*Magnification in microscope).

Table 3
Values of the diameter of single fibers before and after oxidative surface treatments.

Surface treatment	No surface treatment	Electro-chemical oxidation	Thermo-chemical oxidation
Diameter (μm)	7.4 ± 0.5	7.3 ± 0.4	7.3 ± 0.5

two peak components are necessary in order to differentiate sp^2 and sp^3 hybridizations of carbon atoms in carbon materials, either in diamond-like structures [35] or amorphous carbon [36]. The O(1s) peak was fitted according to peak components suggested by Zielke et al. [37] and Lakshminarayanan et al. [38]. The N(1s) peak was fitted according to peak components suggested by Alexander and Jones [39]. The C(1s) peak fitting was done so that the total area of all the oxy-carbonated components could not be higher than the total area of the O(1s) peak and that the total area of all the nitro-carbonated components could not be higher than the total area of the N(1s) peak.

The two liquid phase method was used to measure the surface energy γ_F of the fibers and its dispersive γ_F^D and polar γ_F^P components. The method was described in details by Schultz and Nardin [40]. A single fiber was immersed at a constant speed successively in an alkane and in water, the alkane being superposed to the water (Fig. 1). Several alkanes had to be tested. In this study, octane, nonane, decane, dodecane and hexadecane were used. The electrobalance DCA-322 from Cahn was used to measure the forces applied to the single fiber. The sensitivity was 10^{-6} g and the speed of the displacement of the fiber was 1 mm min^{-1}. As the fiber was immersed in both liquids, the total force applied to it was composed by the buoyancy effect F_B and the tension forces created by the two liquids F_{HA} and F_{HW}. The sample weight was considered compensated by taring prior to measurement.

The two liquid phase method is advantageous because it involves a dynamic wetting. An advancing contact angle and a hysteresis can be determined, which are representative of real surfaces, with different contact angles at equilibrium. The hysteresis assesses the influence of the roughness and the energy

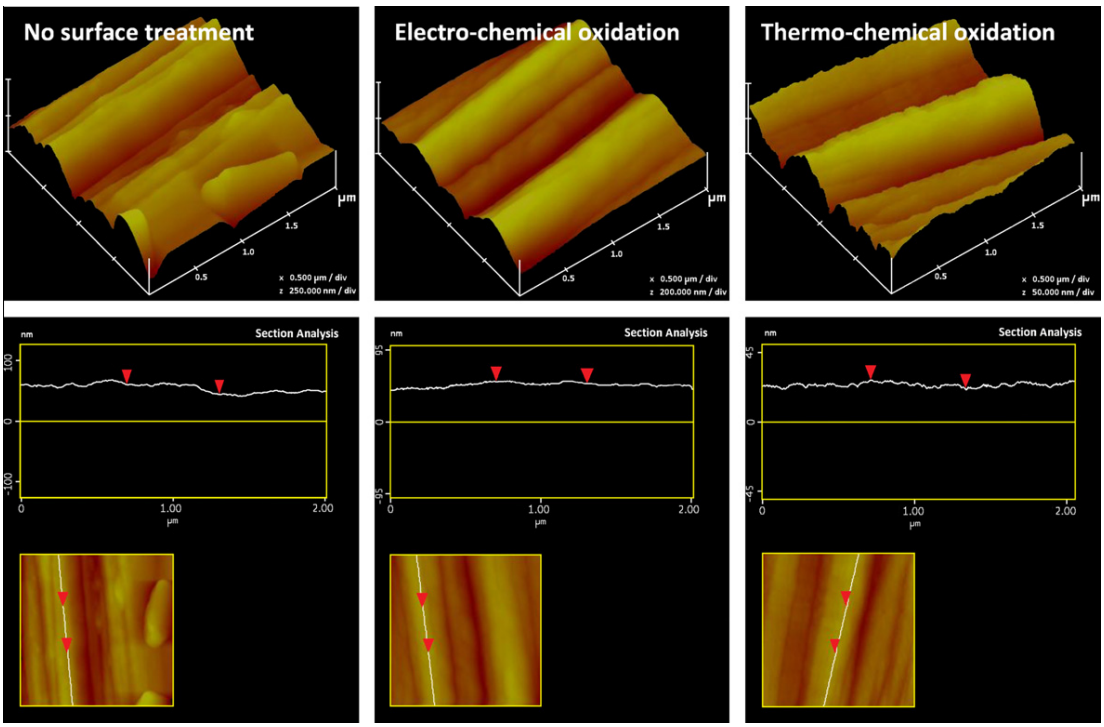

Fig. 3. AFM imaging of the surface of the fibers and roughness of the surface of the fibers, along the fiber axis. (For interpretation of the references to colour in this figure legend, the reader is referred to the web version of this article.)

Table 4
Highlighted summary of surface topography before and after surface treatments.

	No surface treatment	Electro-chemical oxidation	Thermo-chemical oxidation
Height of the ridges (>30 nm)	Reference	Slightly diminished	Significantly diminished
Small Pits (<10 nm)	Very few	Very few	Spread all over the surface
Contamination	Observed contamination	Clean surface	Clean surface

heterogeneity of the surface. Moreover, this method does not require the value of the diameter of the fiber, which is very convenient when a surface treatment changes that value by abrasive treatment or coating of the fiber surface. The only limit associated to that method is a necessity for water to replace the alkane at the surface of the fiber during immersion and for the alkane to replace water during emersion, which is difficult with polar surfaces [41].

The tensile strength of single fibers was measured according to ASTM C1557. The fiber was mounted on a slotted testing tab with the fiber aligned along the center of the tab. The fiber was secured at opposite ends of the slot by an epoxy-based adhesive. Special care was taken so that the fiber was not misaligned and not twisted, as recommended by the ASTM standards. After the adhesive was cured, the ends of the tab were grasped in the grips of a MTS Alliance RT/5 twin screw load frame controlled by the software Testworks 4 and equipped with a 5 N load cell. Four gauge lengths were tested: 6.4, 12.7, 25.4 and 50.8 mm (corresponding to 0.25, 0.5, 1 and 2 inches). A tensile load was applied with a speed of displacement of 0.5, 1, 2 and 4 mm min^{-1} respectively. 30 samples per type of fiber were tested for each gauge length. The diameter of each single fiber was first measured with a digital optical microscope Keyence VH-2500 R at a magnification of ×5000.

2.3. Manufacturing of the composite samples

In the case of vinyl ester composites, Derakane 782 from Ashland Co. was used. 1.5 wt.% of tert-butylperoxybenzoate (initiator) was added and thoroughly mixed by the use of a DAMON/IEC CRU-5000 centrifuge (rotation speed: 3000 rpm, time: 4 min), which also enabled a degassing of the mix, the radical polymerization of vinyl ester resins being inhibited by oxygen. The thermal program for the cure was 1 h at 150 °C.

In the case of epoxy composites, Epon 828 from Hexion Co. was used, which is a DiGlycidyl Ether of Bisphenol A (DGEBA) epoxy resin. 26.4 phr of Epikure W (curing agent) from Hexion Co. were added and thoroughly mixed by the use of the centrifuge (rotation speed: 3000 rpm, time: 4 min). The thermal program for the cure was 2 h at 85 °C followed by 2 h at 149 °C.

Unidirectional composite panels were obtained by winding the carbon fibers around a steel frame and placing them in a two-piece steel mold. The fibers were impregnated with an excess of resin by layup with use of a roller made out of Teflon®. When closing the mold with pressure, the excess of resin was expelled. The dimensions of free space in the mold controlled the dimensions of the composite samples, which was constant. The mold was then placed in a furnace that was digitally controlled, so that the thermal history was identical for all the samples, including the cooling to room temperature after completion of the cure. The volume fraction of fibers was 50%.

2.4. Assessment of the fiber volume concentration and the level of porosity of the composite samples

The level of porosity was measured by acid digestion according to ASTM 3171 in the case of epoxy composites only. Indeed, the vinyl ester matrix could not be digested by that method. Nevertheless, due to the fact that the viscosity of the vinyl ester resin was lower than the viscosity of the epoxy resin, it is assumed that the porosity of the vinyl ester composites was at least as low as for the epoxy composites.

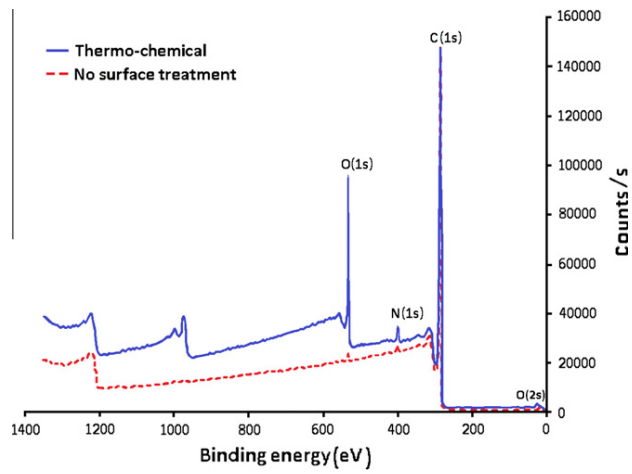

Fig. 4. XPS survey spectra of untreated and thermo-chemically surface treated fibers. (For interpretation of the references to colour in this figure legend, the reader is referred to the web version of this article.)

A MarsX 1200 W microwave was used to bring the nitric acid to a boil. 30 mL of 70% nitric acid were used to digest 1 g of composite. Everything was kept in specifically designed vessels equipped with probes monitoring temperature and pressure. The microwave was set up to reach 130 °C in 15 min and hold at 130 °C for 10 min, allowing a rise in the pressure. The protocol was optimized to digest the matrix completely without damaging the fibers significantly. The fibers were then filtered and rinsed with distilled water and Methyl Ethyl Ketone with the use of a Whatman filter previously dried at 135 °C. The remaining product was dried with the Whatman paper at 135 °C for 1 h before further weight measurements.

Densities of the matrix and the composite samples were measured by the displacement method using water according to ASTM D792. The samples were cleaned with ethyl alcohol and dried before measurement. The density was measured for 20 samples coming from the composite panels and a panel of pure resin that cured separately.

2.5. Testing on unidirectional composites

Short beam shear and flexural tests were done according to ASTM D2344 and ASTM 790-92 respectively. For each carbon fiber–resin system, 10 samples were tested in the case of the

Table 5
Atomic composition of the surface of the fibers measured by XPS analysis.

	C (%)	O (%)	N (%)
No surface treatment	98	2	<1
Electro-chemical surface treatment	88	7	5
Thermo-chemical surface treatment	73	20	3

Table 6
Relative area of each component in the fitting of C(1s), O(1s) and N(1s) peaks, in percentage of the total area of the peak.

	C_{1s}							O_{1s}						N_{1s}			
	Csp^2	Csp^3	C—COOR	C—N	C—O—R, C≡N	C=O	COOR	Ph=O, Ph—C=O	C=O	R—OH, C—O—C	Ph—OH, C—O	H_20 Chem	H_20 Phys	Pyridine	Amines amides nitriles	Pyrrolidine, pyridone	Pyridinium, protonated N
No surface treatment	87	10	0	0	2	1	0	27	30	21	18	3	1	11	3	34	52
Electro-chemical	82	2	2	6	3	3	2	27	12	44	32	5	5	14	32	28	26
Thermo-chemical	76	2	6	2	5	3	6	20	24	14	34	4	4	25	8	30	37

flexural 0° and the flexural 90° tests. The dimensions of the specimens were 127 mm × 12.7 mm × 3.2 mm and the span-to-depth ratio was 16. In the case of the short beam shear test, 2 batches of 10 samples coming from 2 different composite panels were tested. The dimensions of the specimens were 19.2 mm × 6.4 mm × 3.2 mm and the span-to-depth ratio was 4. A MTS Alliance RT/5 twin screw load frame was used with a 5 kN load cell. The testing device was controlled by the software Testworks 4. For the observation of the surface of the fractured composites, a Hitachi S3400 Variable Pressure Scanning Electron Microscope (SEM) was used, in high vacuum and secondary electron mode. The samples were coated with gold and fixed on the sample holder with carbon tape. The acceleration voltage was 20 kV and the intensity of the emission current was 60 μA.

3. Results and discussions

Non surface treated Panex® 35 fibers presented typical grooves in their axis (Fig. 2). Those grooves were formed during the spinning of the PolyAcryloNitrile (PAN) precursor. At the microscopic scale, high magnification pictures showed that no large surface defects were created but it was not possible to discriminate the surfaces regarding the depth of the grooves. Detailed surface topography images were obtained by AFM and are reported hereafter. The cross-section of those fibers being circular, the diameter of single fibers could be measured by image analysis, and 20 values were obtained for each reference. No significant change of the average value of the diameter was observed after the oxidation of the carbon fiber surface (Table 3). A significant scattering was noticed but it was characteristic of the original fibers. The average value matched the data given by the manufacturer.

2 μm × 2 μm surface section of the fibers before and after surface treatment were scanned by AFM. The characteristic features of their surfaces are shown in Fig. 3. The 3D equivalents of the 2D images are given for a better representation of the shape and depth of the features. The topography of the non surface treated fibers was made of 200–400 nm width ridges that were oriented along the fiber axis. The height of those ridges was around 200–250 nm. The surface of the ridges was very smooth. Some grains (contamination) with an average diameter of several hundred nanometers were randomly found on the surface, constituting pyrolitic by-products produced during the carbonization step. After the electro-chemical surface treatment, the ridges appeared to be similar but their height slightly decreased to 150–200 nm. The contamination was removed. Electro-chemical surface treatments typically create microporosity (the diameter of the holes being inferior to 2 nm) at the surface of carbon fibers [23,24]. Although the electro-chemical surface treatment created 7% of oxygen atomic content on the surface, there was no creation of roughness. In the case of the thermo-chemical surface treatment, the height of the ridges was diminished to around 100–150 nm and a secondary structure made of smaller pits (<10 nm) was generated. The contamination was also removed after the thermo-chemical surface treatment. The observed surface topography features obtained from ten AFM images are summarized in Table 4. The topography looked similar between non-surface treated fibers and electro-chemically surface treated fibers with the exception of a slight decrease of the height of the ridges and the contamination. After the thermo-chemical surface treatment, the original topography was eroded (ridges) and replaced by pits with much smaller dimension. That effect was also reported by Jin et al. [34]. Gao et al. [42] claimed that only the fiber surface roughness that is under a few tens of nanometers contributes to interfacial adhesion through mechanical interlocking. Therefore, more mechanical interlocking with the matrix should

be generated by the surface of the thermo-chemically oxidized fibers, thus improving interfacial adhesion, but it is necessary to verify that this change in topography is not responsible for a loss of the mechanical properties of the fibers, which will be investigated hereafter.

The survey spectra of untreated and thermo-chemically surface treated fibers are displayed in Fig. 4. The intensity of the signals was normalized to the intensity of the C(1s) peak of the surface treated fibers. The only elements present at the surface of the fibers were carbon, oxygen and nitrogen. As expected, the signal of the O(1s) peak is weak in the case of untreated fibers and strong in the case of surface treated fibers. The atomic composition of the surface of the fibers is given in Table 5. The oxygen content was increased from 2% to 7% after the industrial electro-chemical surface treatment and up to 20% after the thermo-chemical surface treatment. It can be noticed that the presence of nitrogen was barely detected at the surface of the untreated fibers, which can be due to the fact that it is covered with highly graphitic residue coming from the graphitization of the fiber. The nitrogen content increased after the electro-chemical surface treatment up to 5%. It is known that commercial surface treatments are optimized for epoxy resin applications [43], so the creation of amines groups at the surface of the fiber in order to create covalent bonding is targeted. After the thermo-chemical surface treatment, the atomic content of nitrogen was only 3%. A fitting of the C(1s), O(1s) and N(1s) peaks was done in order to identify the nature of the chemical functionalities that were created at the surface of the fibers (Table 6). As an example, the fitting of the peaks corresponding to the spectrum of the thermo-chemically surface treated fibers is displayed in Fig. 5.The surface chemistry of the non surface treated fibers was made of low concentrations of alcohol, ether, epoxide, carbonyl and lactone functionalities. After the electro-chemical surface treatment, some ether and epoxide functionalities, hydroxyl and carbonyl groups and a small amount of carboxylic acid and lactone functionalities were generated. The fitting of the O(1s) peak revealed that the majority of the C—O bonds were belonging to ether, epoxide or alcohol functionalities. The surface treatment produced some amines, apart of some nitrogen that was incorporated in the graphitic structure of the fiber. A significant amount of water was adsorbed at the surface, which can affect interfacial adhesion. The thermo-chemical surface treatment created preferentially hydroxyl groups (phenol functionalities in majority as shown by the fitting of the O(1s) peak) and carboxylic acid functionalities. Some carbonyl groups were found as well. Although a limited amount of nitrogen was incorporated in the graphitic structure, barely any amine was generated on the surface. The carbon material that constituted the outer layers of the fiber became less graphitic because the creation of more functionalities induced more defects in the lattice. A significant amount of adsorbed water was observed for both surface treatments, but that amount was reduced in the case of the thermo-chemical treatment. The fitting of the peaks was combined to the atomic percentage of each element in order to compare the relative surface concentrations of the three main types of functionalities that were generated (carboxylic acid, carbonyl group, hydroxyl group) (Fig. 6). The concentration of carbonyl groups existing at the surface of the non surface treated fibers was arbitrarily chosen to be equal to 1 and the values of the other densities were calculated proportionally. The electro-chemical surface treatment generated the three types of functionalities with equivalent concentrations, thus not considered very discriminative. In comparison, the thermo-chemical surface treatment preferentially created hydroxyl groups and carboxylic acids, the concentration of carbonyl groups being significantly lower. The thermo-chemical surface treatment functionalized the fiber surface with a narrow distribution of moieties centered on desired chemical groups which are strategic for the improvement of interfacial adhesion in carbon fiber composites because it has been demonstrated that hydroxyl groups and carboxylic acids create covalent bonding with epoxy resins [44,45].

Since the size of the tow was large (50 k), it was necessary to assess the homogeneity of the surface treatment. The tow was separated in the middle in two equal half tows and the surface that was

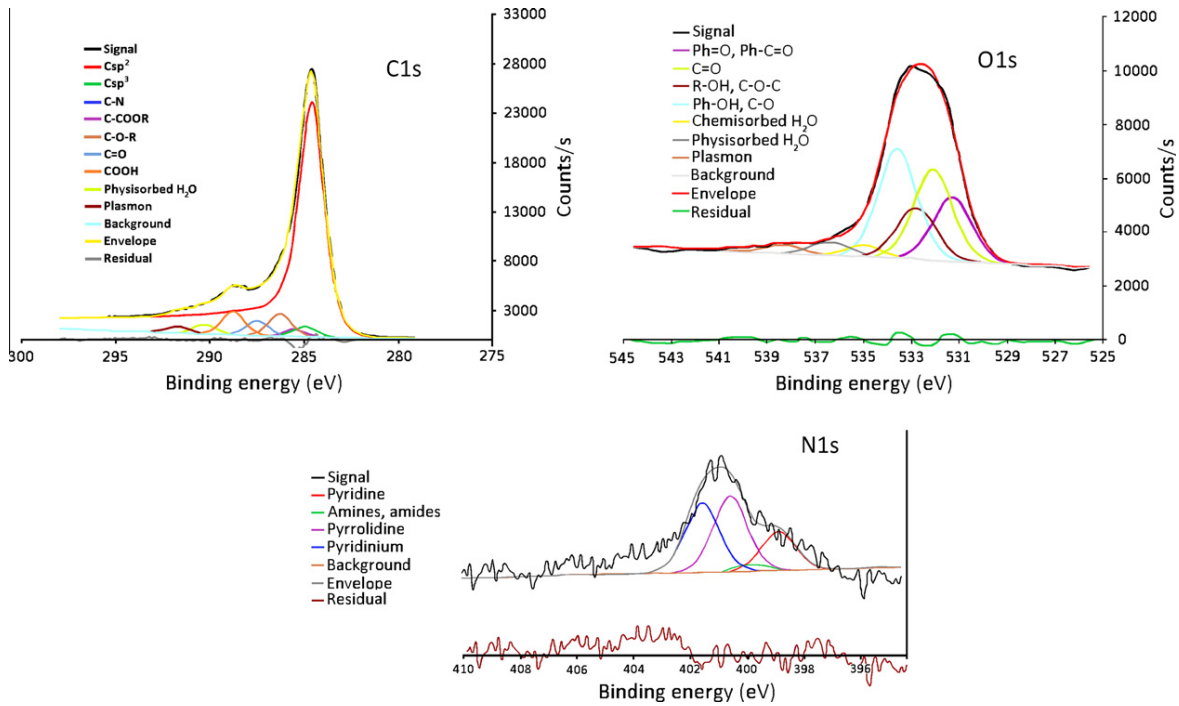

Fig. 5. Fitting of the C(1s), O(1s) and N(1s) peaks of the spectrum corresponding to the thermo-chemically surface treated fibers. (For interpretation of the references to colour in this figure legend, the reader is referred to the web version of this article.)

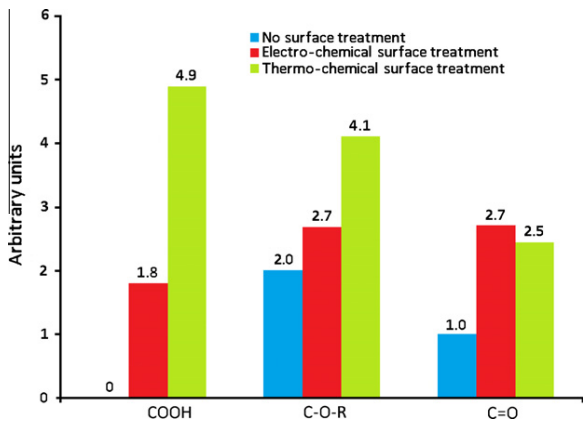

Fig. 6. Comparison of the relative densities of functionalities existing at the surface of the non treated and surface treated fibers. (For interpretation of the references to colour in this figure legend, the reader is referred to the web version of this article.)

Table 7
Homogeneity of the thermo-chemical surface treatment in the carbon fiber tow, oxygen content.

	C (%)	O (%)	N (%)
External part of the tow	73	20	3
Center of the tow	73	20	3

originally in the center of the tow was analyzed by XPS. The concentration of oxygen was the same as the concentration corresponding to single fibers located at the external part of the tow (Table 7).

The fitting of the C(1s), O(1s) and N(1s) peaks revealed that the surface chemistry generated at the center of the tow is equivalent to that created at the external part. As the surface treatment was continuous, an XPS analysis was carried out on several samples being separated by a few meters in the spool. It was concluded that the treatment was consistent, with a concentration of oxygen remaining relatively stable with an atomic concentration of 19–20%. The fitting of the C(1s), O(1s) and N(1s) peaks revealed that the generated surface chemistry was also consistent.

Since the oxygen content of the fiber surface increased sharply after both surface treatments, assessing its influence on the evolution of the surface energy was relevant. The typical curve given by the electrobalance with the two liquid phase method, in the case of a non surface treated single fiber and a thermo-chemically surface treated single fiber, with a dodecane–water system, is given in Fig. 7. Each time that the single fiber crosses a different phase, a variation of force is first recorded, and then a plateau is reached. Knowing the diameter of the fiber, it was possible to calculate the contact angle, both for immersion and emersion.

For a non-oxidized fiber, the wetting by water was difficult, the immersion contact angle being 78°. The emersion contact angle in water was 50°. The hysteresis was then 28°. After the thermo-chemical surface treatment, the wetting by water was slightly improved, as the immersion contact angle was 76°. The emersion contact angle in water was 41°. The hysteresis was then 35°. In general the hysteresis can be created by the roughness, the heterogeneity of the surface chemistry, the swelling of the surface of the sample by penetration of some of the liquids in the sample or by the reorganization of the surface functionalities [46]. In the present case, the topography of the surface and the heterogeneity of the surface energy of carbon fibers seemed to be mainly responsible for the hysteresis, even for non-oxidized fibers. The calculation of the advancing dispersive (γ^D) and polar (γ^P) components of the surface energy γ was done for the three types of fibers, using the different alkanes listed in the Section 2, and the results are presented in Table 8.

The surface energy of the electro-chemically oxidized fibers was barely higher than the one of the non surface treated fibers, which was expected considering that the oxygen content measured by XPS was very low. Indeed, the polar component increased slightly but not enough to convey a dramatic increase of the surface energy of the fiber. In comparison, the polar component of the surface energy of the fibers that were thermo-chemically surface treated increased sharply, which resulted in an overall significant increase of the surface energy. In all cases, the dispersive component

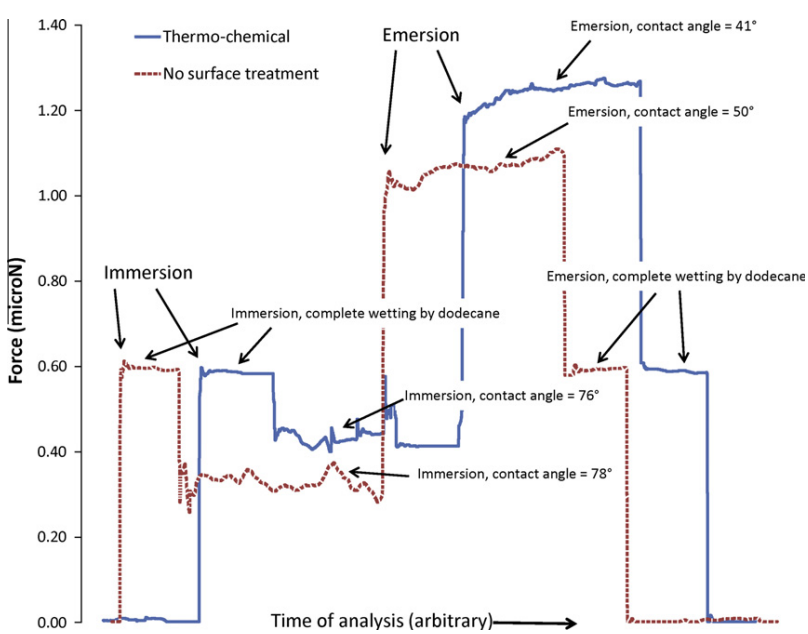

Fig. 7. Two liquid phase method, non surface treated and thermo-chemically surface treated fibers, dodecane–water system. (For interpretation of the references to colour in this figure legend, the reader is referred to the web version of this article.)

Table 8
Dispersive γ^D and polar γ^P components of the surface energy of the fibers before and after surface treatments calculated from advancing contact angle measurements.

	γ^D (mJ.m^2)	γ^P (mJ.m^2)	γ (mJ.m^2)
No surface treatment	49 ± 15	15 ± 1	64 ± 15
Electro-chemical	49 ± 12	19 ± 3	68 ± 12
Thermo-chemical	54 ± 17	26 ± 4	80 ± 17

remained at the same value. The fact that the surface energy of the thermo-chemically surface treated fibers is higher will improve the wetting of the fibers by the matrix (which is a necessary but not sufficient condition in order to obtain high adhesion strength) and will increase the density of physical interactions at the interface, which will have an influence on the interfacial adhesion. The main surface properties that monitor interfacial adhesion have been characterized.

Another parameter that must be checked is the evolution of the mechanical properties of the single fibers after surface treatment. A loss of the mechanical properties is indeed not acceptable. The tensile strength of the fiber was measured before and after surface treatment as well. The tensile strength of the single fibers for each gauge length is given in Table 9. The tensile modulus remained unchanged and was equal to the value given by the manufacturer so it was not reported. The tensile strength of the electro-chemical surface treated fibers was slightly lower than the value reported in Table 1, which is related to sized fibers. The sizing protects the fiber against damage generated by friction of one single fiber against another during handling. Then the properties of sized fibers are potentially unaffected until testing. Moreover, the value of the tensile strength given by the manufacturer was measured with a tow, not with single fibers. A trend showing an increase of the tensile strength after the surface treatments was noticed, even if the average values were not perfectly statistically different when considering their standard deviation, and this was more pronounced in the case of the thermo-chemical surface treatment.

Because the tensile strength depends on the gauge length (the probability of having a flaw leading to the breakage being higher with a longer gauge), it is necessary to determine parameters related to the tensile properties that are independent of the gauge length, i.e. the Weibull modulus and the scale parameter. The determination of the Weibull modulus and the scale parameter was done accordingly to Asloun et al. [47], i.e. by plotting the neperian logarithm of the average tensile strength for each gauge length in function of the neperian logarithm of the gauge length (Fig. 8 and Table 9). In their approach, the average tensile strength of the fiber σ is related to the gauge length l according to Eq. (1), with m and σ_0 being the Weibull modulus and the scale parameter respectively, and Γ being the gamma function:

$$\ln\sigma = \frac{-1}{m}\ln l + \ln\left[\sigma_0\Gamma\left(1+\frac{1}{m}\right)\right] \quad (1)$$

The value of the Weibull modulus m and the ultimate tensile strength σ_0 can be easily determined with Fig. 8. This method was shown to be more appropriate than a regular two or three

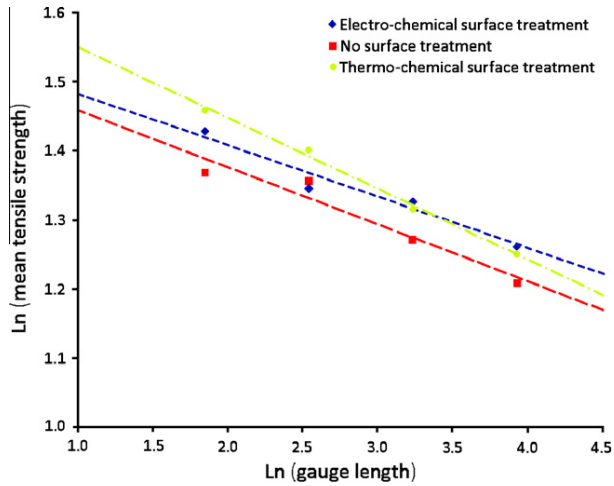

Fig. 8. Determination of the Weibull modulus and the scale parameter. (For interpretation of the references to colour in this figure legend, the reader is referred to the web version of this article.)

parameter Weibull analysis, because the latter gave values of the Weibull modulus and the scale parameter that were depending on the gauge length.

The fibers that were electro-chemically surface treated appeared to be the less sensitive to the gauge length (higher value of the Weibull modulus). That can be explained by a higher density of flaws. The ultimate tensile strength was similar to that of untreated fibers. The nature of the flaws is different though and the break of the fibers might not follow the same mechanism. Indeed, oxidative surface treatments create defects (pits) in the first graphitic layers on the surface but also remove the weak boundary layers of graphitic material produced by the graphitization step during the manufacturing of the fiber. That may explain why the tensile strength of untreated fibers was generally lower than the tensile strength of electro-chemically surface treated fibers. The thermo-chemical surface treatment yielded the lowest value of the Weibull modulus and the highest ultimate strength. It seems that the thermo-oxidative surface treatment presented here, within the experimental conditions used, induced a healing of the carbon fiber surface by removing surface imperfections and replacing them with flaws of smaller amplitudes. The AFM images presented earlier show that the electro-chemical surface treatment only slightly changed the topography of the fibers, preserving a rough surface with defects of a larger amplitude (and eventually more stress at the tip of those defects), which may have made up for the gain obtained with the removal of some of the weak boundary layers originally present at the surface of the fiber. The benefit of removing the weak boundary layers reached its full potential with the thermo-chemical surface treatment, with the erosion of the ridges. Last but not least, it is important to remind that the manufacture of the samples also discriminates toward the most fragile single fibers, creating a pre-selection of the single fibers that has

Table 9
Tensile strength of single fibers and Weibull parameters before and after surface treatments.

Surface treatment	Tensile strength (MPa)	Gauge length in mm (inch)				Weibull modulus m	Scale parameter σ_0 (MPa)
		6.4 (0.25)	12.7 (0.5)	25.4 (1)	50.8 (2)		
No surface treatment	Average value	3930	3875	3565	3351	12.346	4952
	Standard deviation	421	386	407	434		
Electro-chemical surface treatment	Average value	4171	3847	3764	3530	13.333	4843
	Standard deviation	365	441	379	386		
Thermo-chemical surface treatment	Average value	4302	4061	3730	3496	9.901	5421
	Standard deviation	414	372	359	400		

Table 10
Measurement of the level of porosity in the epoxy-based composites.

Surface treatment	Fiber volume fraction (%)	Void volume fraction (%)
No surface treatment	50.2	1.9
Electro-chemical surface treatment	51.6	1.5
Thermo-chemical surface treatment	51.2	1.8

an obvious influence on the final results. The decrease of the tensile strength because of the presence of defects at the surface of the single fiber, and then the healing of those defects after surface treatment, are underestimated because of that pre-selection.

In the case of the thermo-chemical surface treatment, the surface density of strategic functionalities and the surface energy were higher and the tensile properties of the single filament were better. The topography created by the thermo-chemical oxidation was also more efficient for providing mechanical interlocking with the matrix. The accumulation of those parameters is directly influencing interfacial adhesion. Therefore, the mechanical properties of unidirectional composites were measured in order to assess the potential change of those properties with a change of the surface properties of the fibers.

The porosity of composite materials has an imperative effect on their mechanical performance. It was measured by acid digestion to make sure that it was remaining at acceptable levels, that is to say less than 2% in volume fraction. The fiber volume fraction and the porosity corresponding to the epoxy composites made with the three types of fiber are presented in Table 10.

The vinyl-ester composites could not be digested in boiling nitric acid, as vinyl ester resins are designed to be chemically resistant. As mentioned earlier, with the viscosity of the vinyl ester resin being lower than the viscosity of the epoxy mix during the manufacture of the composite panels, the level of porosity was assumed at least as low as in the epoxy composites. With an acceptable level of porosity in the composite samples, a potential change of their mechanical properties could be linked to a modification of the interfacial properties.

The 90° and 0° flexural properties and the values of the interlaminar shear strength obtained before and after surface treatment are reported in Table 11. Drzal and Madhukar [48] showed that the property of a unidirectional composite most sensitive to interfacial adhesion is the 90° flexural strength. When it comes to the vinyl-ester composites, a clear increase of the 90° flexural strength was noticed after the electro-chemical surface treatment (+58%) and the thermo-chemical surface treatment (+116%) in comparison to untreated fibers, the modulus of the composites remaining the same. All the tested coupons broke according to a tensile failure mode. A SEM observation of the fracture profiles is given in Fig. 9. In the case of untreated fibers, the profile presented a brush like aspect, with long fibers that were individually separated, randomly oriented and without matrix remaining on their surface, which is typical of an interfacial failure. With electro-chemically surface treated fibers, the fracture profile still had a brush like aspect with naked fibers, so the rupture mode was still interfacial. Removing the weak boundary layers and generating some oxygen-containing functionalities at the surface of the fibers increased the density of physical interactions between the fiber surface and the matrix (and thus improved the wetting of the fibers by the matrix). Nevertheless, the density of interactions at the interface was still too low to prevent an interfacial failure in the composite. With thermo-chemically surface treated fibers, the fracture was flatter, showing fewer fibers individually separated. Some pieces of matrix could be randomly seen at the surface of the fibers but the amount was still far from what can generally be seen with a cohesive rupture. It appeared that the rupture mode switched slightly from a pure interfacial rupture mode to a mixed mode interfacial/cohesive rupture. The 0° flexural strength, which is much less sensitive to the interface properties than the 90° flexural strength and more sensitive to the mechanical properties of the fibers, did not increase significantly. The modulus was also the same for the three composites. All the tested coupons broke according to a compression failure mode but some obvious interlaminar shear failure mode was also noticed in the case of untreated fibers. The fracture profile of the zone under tension during the test can also indicate the level of interfacial adhesion in the composite (Fig. 10). In the case of untreated fibers, long protruding fibers without matrix on their surface were noticed, which again is a clear proof of poor interfacial adhesion. With the electro-chemical surface treatment, the length of the protruding fibers was slightly reduced and some bundles of fibers were noticed. Clear interfacial failure could still be seen. In the case of the thermo-chemical surface treatment, more resin could be seen around the fibers (picture with a magnification of ×500), with the protruding length also reduced. Again some bundles of fibers were randomly observed, with more matrix around the fibers, but the failure was again clearly interfacial. It was then obvious that there was an increase of interfacial adhesion that was greater after the thermo-chemical surface treatment but its level was still too low to induce a change of the rupture mode from interfacial to cohesive. The values of the interlaminar shear strength increased by +17% with the electro-chemical surface treatment and by +25% with the thermo-chemical surface treatment. All the tested coupons broke according to an interlaminar shear failure mode. The interlaminar shear strength is sensitive to the mechanical properties of the matrix (toughness, shear modulus), the level of porosity and the level of interfacial adhesion. Since the same matrix was used for all the samples and the level of porosity was low, the increase was attributed to the improvement of interfacial adhesion.

This study also highlighted that in the case of carbon fiber–vinyl ester composites, an optimized oxidation of the carbon fiber surface with a high density of oxygen-containing surface functionalities cannot bring the level of interactions that is necessary to

Table 11
Mechanical properties of vinyl ester and epoxy composites.

		No surface treatment	Electro-chemical surface treatment	Thermo-chemical surface treatment
Derakane 782	Flex 90° strength (MPa)	12 ± 2	19 ± 3	26 ± 4
	Flex 90° modulus (GPa)	5.9 ± 0.1	5.9 ± 0.1	5.9 ± 0.1
	Flex 0° strength (MPa)	1188 ± 109	1254 ± 174	1239 ± 98
	Flex 0° modulus (GPa)	117.6 ± 1.6	115.0 ± 2.2	116.9 ± 2.6
	ILSS (MPa) (2 batches from 2 different panels)	57 ± 3, 59 ± 2	69 ± 4, 68 ± 3	74 ± 4, 72 ± 4
Epon 828	Flex 90° strength (MPa)	34 ± 3	81 ± 7	97 ± 8
	Flex 90° modulus (GPa)	7.3 ± 0.1	7.3 ± 0.1	7.4 ± 0.1
	Flex 0° strength (MPa)	981 ± 102	1099 ± 88	1133 ± 44
	Flex 0° modulus (GPa)	97.2 ± 1.7	96.2 ± 2.0	96.1 ± 2.2
	ILSS (MPa) (2 batches from 2 different panels)	52 ± 3, 51 ± 3	72 ± 4, 73 ± 3	85 ± 3, 87 ± 4

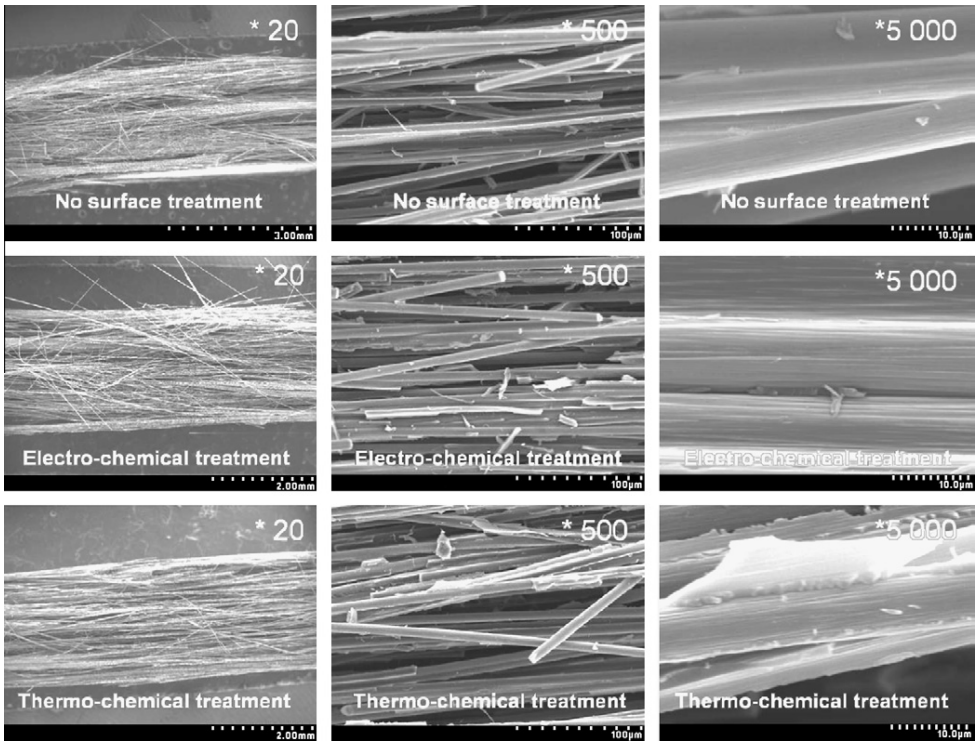

Fig. 9. Fracture profile of vinyl ester composites after a flexural 90° test. (*Magnification in microscope).

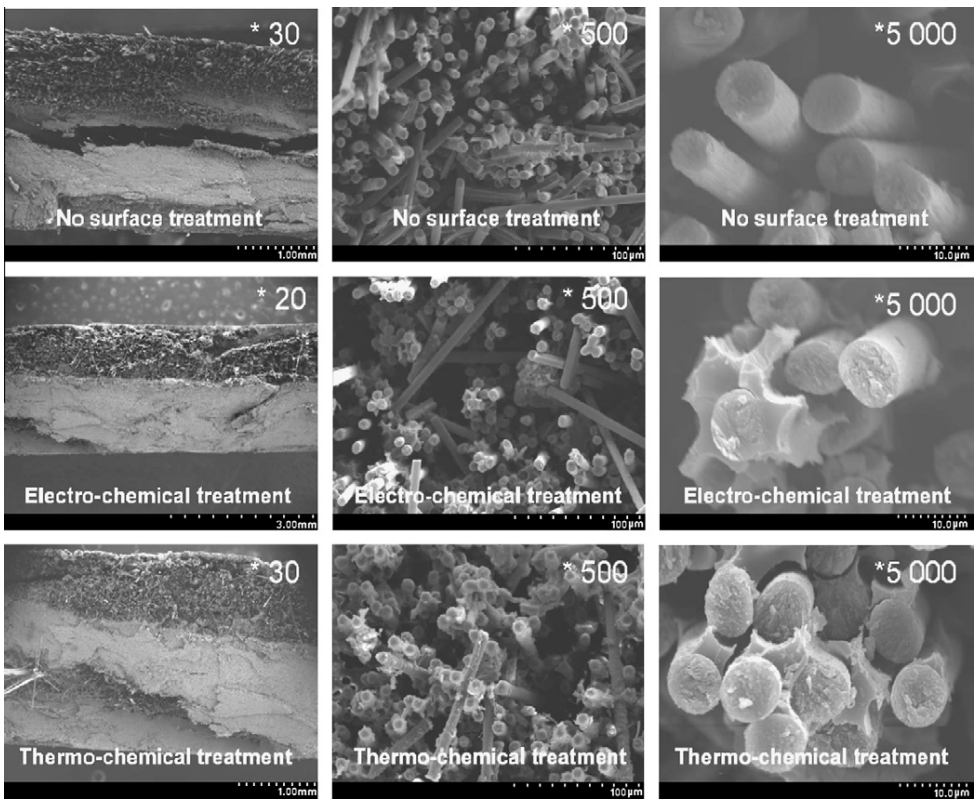

Fig. 10. Fracture profile of vinyl ester composites after a flexural 0° test. (*Magnification in microscope).

obtain mechanical properties that would be equivalent to those of epoxy-based composites. For vinyl ester composites, the surface chemistry generated at the surface of the fibers has an influence on both the type of interactions that are generated at the interface

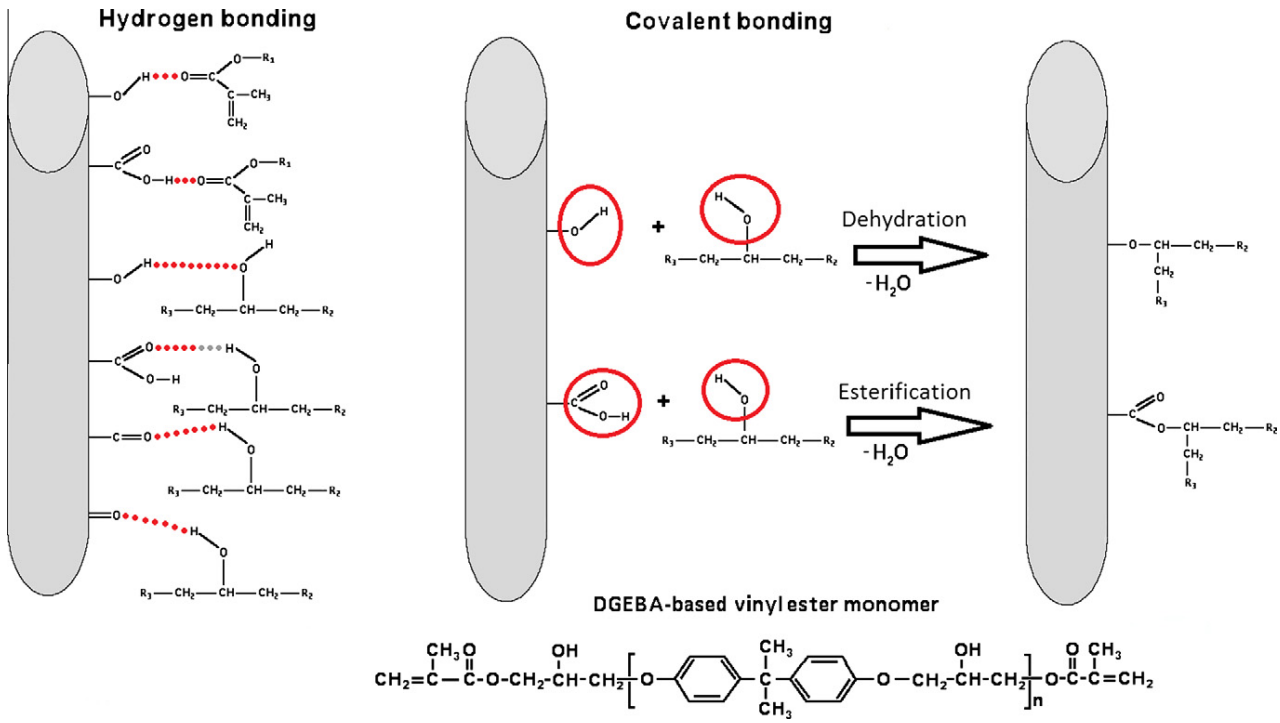

Fig. 11. Hydrogen bonding and chemical interactions between the carbon fiber surface and a DiGlycidyl Ether of Bisphenol A (DGEBA)-based vinyl ester monomer. (For interpretation of the references to colour in this figure legend, the reader is referred to the web version of this article.)

and the creation of a thick interphase with a fraction conversion lower than the fraction conversion of the bulk. Indeed, Dirand et al. [49] showed that the surface chemistry of a material in contact with a vinyl ester resin played a major role in the polymerization of that vinyl ester in the vicinity of its surface, leading to interphases with very large thicknesses, of several hundreds of microns in some cases. More investigation is also needed to understand the role of styrene in the interactions existing at the interface. Indeed, its surface energy (33 mJ m^2) is lower than the surface energy of the vinyl ester monomers (generally above 40 mJ m^2 [50,51]), which can potentially lead to a preferential adsorption of styrene at the surface of the fibers, especially considering the π-π interactions that can be created with the graphitic structure of the fiber surface. Such a preferential adsorption had recently been suggested by molecular dynamics simulations [52]. If the oxygen-containing functionalities present at the surface of the carbon fibers could have the potential to create strong physical interactions like hydrogen bonding and eventually covalent bonding with the ester and alcohol functionalities existing in the epoxy-based vinyl ester monomers present in Derakane vinyl ester resins (Fig. 11), that potential would be ruined by a layer of adsorbed styrene at the surface of the fibers. All in all, the chemistry created by oxidative treatments is not adapted to the radical polymerization of vinyl ester resins. It is confirmed by the fact that better values of the 90° flexural strength and of the interlaminar shear strength have been reported with the use of reactive sizings [53] or the creation of Interpenetrating Polymer Networks (IPNs) with a reactive epoxy sizing [54], which can prevent the preferential adsorption of styrene at the surface of the fibers and for which covalent bonding with the carbon fiber surface is realized. The thermo-chemical surface treatment presented here still represents an optimized surface for the grafting of coupling agents or reactive sizings, as it provides a high density of hydroxyl groups and carboxylic acids, which are usually the functionalities used for grafting [55]. A synergy between this surface treatment and the use of an appropriate coupling agent or reactive sizing may lead to very high values of interfacial adhesion.

The 90° and 0° flexural properties and the values of the interlaminar shear strength of the epoxy-based composites are also reported in Table 11. A sharper increase of the 90° flexural strength was measured in comparison to the vinyl ester composites, both for the electro-chemical surface treatment (+138%) and the thermo-chemical surface treatment (+185%). The flexural moduli of the composites were the same and all the tested coupons broke according to a tensile failure mode. The interfacial adhesion was then greatly improved by surface treatment and particularly by the thermo-chemical surface treatment. A SEM image of the fracture profiles is given in Fig. 12. With untreated fibers, the fracture profile had a brush like aspect and no matrix was observed at the surface of the fibers but it was still a little less fuzzy than the profile obtained with the vinyl ester resin. This profile proved that the interfacial adhesion is low. With similar level of physical interactions at the interface, the interfacial adhesion will still be worse in the case of vinyl ester resins because of the influence of the cure volume shrinkage (5–9% as compared to 2–3% for epoxy resins) [9]. With the electro-chemical surface treatment, the profile was flat, with no fiber individually separated (only bundles), and some pieces of matrix were remaining at the surface of the fibers, without covering them completely. With a low density of oxygen-containing functionalities the rupture mode was already switching from a pure interfacial failure to a mixed mode interfacial/cohesive. Even a limited density of covalent bonding induced by the hydroxyl groups and the carboxylic acids located at the surface of the fiber improved the interfacial adhesion tremendously. The thermo-chemical surface treatment led to the flattest fracture profile, with almost no fiber protruding, just a few bundles. The amount of resin remaining at the surface was large, which indicated a pure cohesive rupture mode. The interfacial adhesion was quite strong. Regarding the 0° flexural properties, a significant increase was only noticed with the use of the thermo-chemical surface treatment.

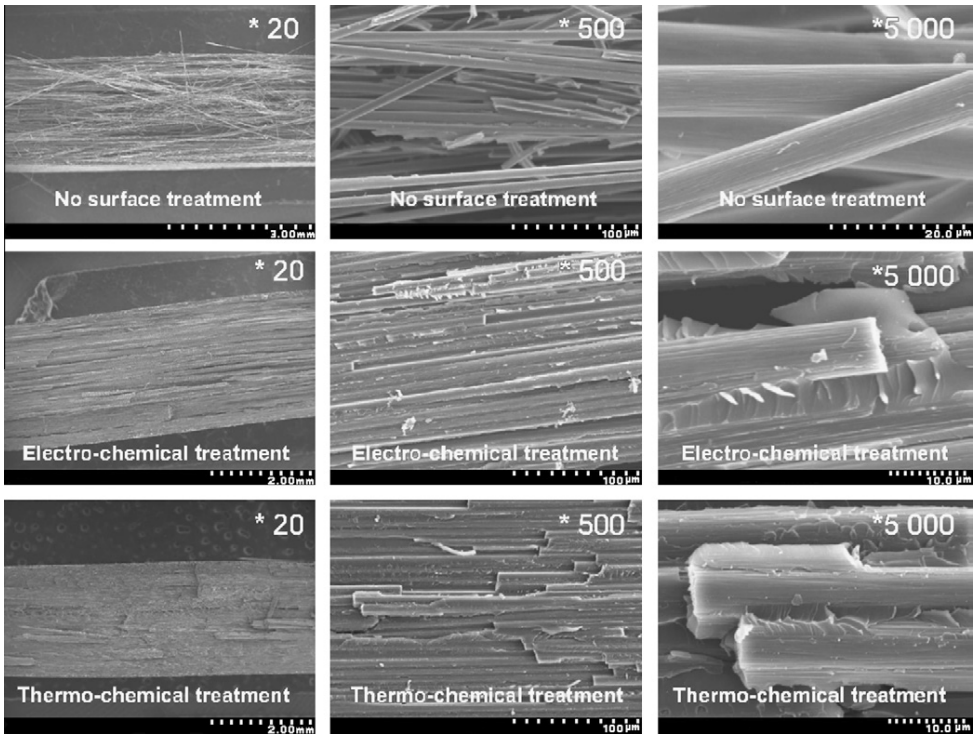

Fig. 12. Fracture profile of epoxy composites after a flexural 90° test. (*Magnification in microscope).

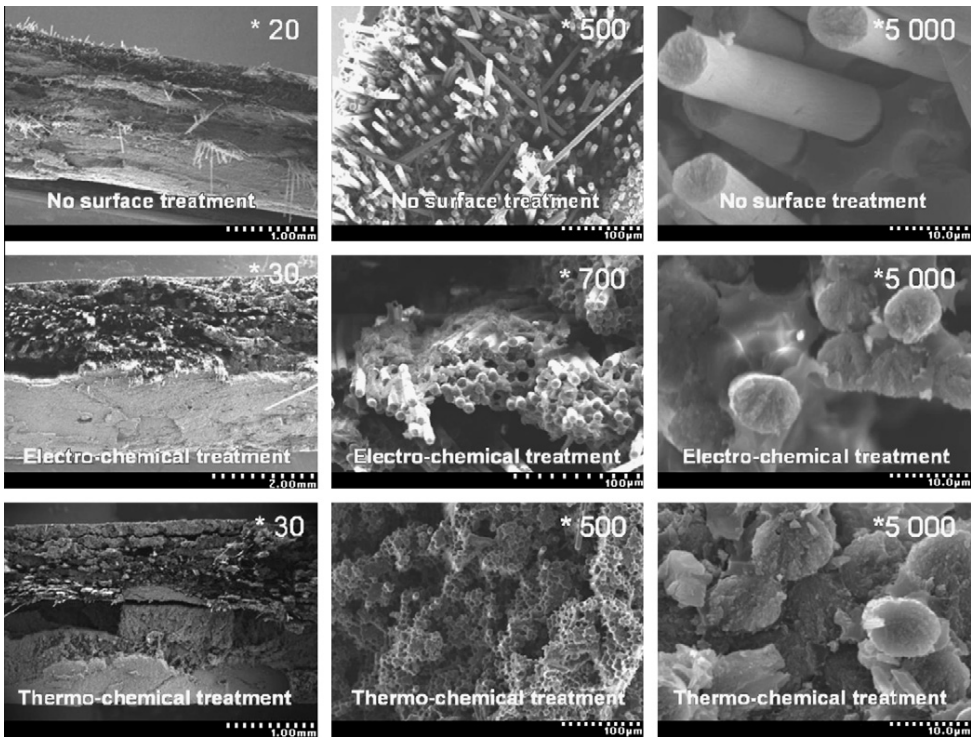

Fig. 13. Fracture profile of epoxy composites after a flexural 0° test. (*Magnification in microscope).

The modulus was the same for the three composites. All the tested coupons broke according to a compression failure mode but some obvious interlaminar shear failure mode was also noticed in the case of untreated fibers. An increase in interfacial adhesion increases both the tensile and compressive strength of composites so it is expected to see a change in the 0° flexural strength. To observe this effect, the increase in interfacial adhesion has to be sharp. The corresponding fracture profiles are presented in

Fig. 13. With untreated fibers, the zone that was under tension showed long and naked protruding fibers, with a clear interface failure located at their base. The interfacial adhesion was low. With the electro-chemical surface treatment, the length of the protruding fibers was considerably reduced, and a lot of fibers stayed stuck together in bundles. With the thermo-chemical surface treatment, no fiber was protruding at all, which indicated a pure cohesive rupture mode. The value of the interlaminar shear strength was in accordance with the increase in interfacial adhesion. It increased to +38% with the electro-chemical surface treatment and to +65% with the thermo-chemical surface treatment. All the tested coupons broke according to an interlaminar shear failure mode.

4. Conclusions

Chemically and physically modified carbon fiber surfaces using two different surface treatments were characterized and the effect on interfacial adhesion was investigated. The thermo-chemical surface treatment generated homogeneously and consistently a higher concentration of hydroxyl groups and carboxylic acid functionalities at the surface of the fibers, thus increasing the surface energy of the fiber, which led to a better wetting of the fibers by the matrix. A topography adapted to the transfer of load from the matrix to the fiber by mechanical interlocking was created as well, and it did not lower the tensile properties of the single fibers. Some healing effect was even suggested by an analysis of the values of the tensile strength at different gauge lengths. The increase of interfacial adhesion with vinyl ester resin was limited. But the high density of hydroxyl groups and carboxylic acids is suitable for the grafting of adapted coupling agents and reactive sizings. In the case of epoxy resins, the increase of interfacial adhesion was really sharp, and the fibers could be directly used after surface treatment for optimal properties. Depending on the application, the surface can also interact strongly with an epoxy compatible sizing.

Acknowledgment

This research was sponsored by the U.S. Department of Energy, Assistant Secretary for Energy Efficiency and Renewable Energy, Office of Vehicle Technologies, as part of the Lightweighting Materials Program. A part of this research was done through the Oak Ridge National Laboratory's High Temperature Materials Laboratory User Program, sponsored by the U. S. Department of Energy, Office of Energy Efficiency and Renewable Energy, Vehicle Technologies Program and through the Shared Research Equipment (SHaRE) User Facility operated for the U. S. Department of Energy Office of Science by the Oak Ridge National Laboratory. Authors would like to thank Mr. Truman Bond and ReMax Lo. for their indispensible contribution to the development of the surface treatment technology. Zoltek, Hexion and Ashland Co. are sincerely thanked for providing the carbon fibers, the epoxy resin and its curing agent and the vinyl ester resin respectively. Mr. Ronny Lomax is thanked for his contribution in the acid digestion of the epoxy based composites. Ms. Laura Poland and Mr. Matthew Warren are sincerely acknowledged for the manufacturing and the testing of the single fiber tensile test coupons. Dr. Tolga Aytug is also acknowledged for his help with AFM imaging.

References

[1] Nardin M, Asloun EM, Schultz J. Physico-chemical interactions between carbon fibers and PEEK. In: Ishida H, editor. Controlled interphases in composites materials. New York: Elsevier; 1990. p. 285–93.
[2] Jennings CW. Surface roughness and bond strength of adhesives. J Adhes 1972;4:25–38.
[3] Raghavendran VK, Drzal LT, Askeland P. Effect of surface oxygen content and roughness on interfacial adhesion in carbon fiber-polycarbonate composites. J Adhes 2002;16:1283–306.
[4] Owens DK, Went RC. Estimation of the surface free energy of polymers. J Appl Polym Sci 1969;13:1741–7.
[5] Fowkes FM. Role of acid–base interfacial bonding in adhesion. J Adhes Sci Technol 1987;1:7–27.
[6] Hook KJ, Agrawal RK, Drzal LT. Effects of microvawe processing on fiber–matrix adhesion. 2. Enhanced chemical bonding epoxy to carbon–fibers. J Adhes 1990;32:157–70.
[7] Bikerman JJ. The science of adhesive joints. New York: Academic Press; 1961.
[8] Paiva MC, Nardin M, Bernardo CA, Schultz J. Influence of thermal history on the results of fragmentation tests on high-modulus carbon–fiber/polycarbonate model composites. Compos Sci Technol 1997;57:839–43.
[9] Vautard F, Xu L, Drzal LT. Carbon fiber–vinyl ester interfacial adhesion improvement by the use of an epoxy coating. In: Daniel IM, Gdoutos EE, Rajapakse Y, editors. Major accomplishment in composite materials and sandwiches structures: an anthology of ONR sponsored research. Springer; 2009. p. 27–50.
[10] Drzal LT, Rich MJ, Lloyd PF. Adhesion of graphite fibers to epoxy matrices: I. The role of fiber surface treatment. J Adhes 1982;16:1–30.
[11] Weitzsacker CL, Xie M, Drzal LT. Using XPS to investigate fiber/matrix chemical interactions in carbon fiber reinforced composites. Surf Interface Anal 1997;25:25–53.
[12] Bascom WD, Yon KJ, Jensen RM, Cordner L. The adhesion of carbon fibers to thermosets and thermoplastic polymers. J Adhes 1991;34:79–98.
[13] Park SJ, Kim MH. Effect of acidic anode treatment on carbon fibers for increasing fiber–matrix adhesion and its relationship to interlaminar shear strength of composites. J Mater Sci 2000;35:1901–5.
[14] Gulyás J, Földes E, Lázár A, Pukánsky B. Electrochemical oxidation of carbon fibers: surface chemistry and adhesion. Compos A-Appl S 2001;32:353–60.
[15] Proctor A, Sherwood PMA. X-ray photoelectron spectroscopic studies of carbon fiber surfaces-II the effect of electrochemical treatment. Carbon 1983;21:53–9.
[16] Bismarck A, Kumru ME, Springer J, Simitzis J. Surface properties of PAN-based carbon fibers tuned by anodic oxidation in different alkaline electrolyte systems. Appl Surf Sci 1999;143:45–55.
[17] Kozlowski C, Sherwood PMA. X-ray photoelectron spectroscopic studies of carbon fibre surfaces-VII Electrochemical treatment in ammonium salt electrolytes. Carbon 1986;24:357–63.
[18] Harvey J, Kozlowski C, Sherwood PMA. X-ray photoelectron spectroscopic studies of carbon fibre surfaces Part 6 Pilot plant surface treatment and epoxy resin composites. J Mater Sci 1987;22:1585–96.
[19] Waseem SF, Gardner SD, He GR, Jiang WB, Pittman U. Adhesion and surface analysis of carbon fibres electrochemically oxidized in aqueous potassium nitrate. J Mater Sci 1998;33:3151–62.
[20] Alexander MR, Jones FR. Effect of electrolytic oxidation upon the surface chemistry of type a carbon fibers-Part I. X-ray Photoelectron Spec. Carbon 1996;32:1093–102.
[21] Vickers PE, Watts JF, Perruchot C, Chehimi MM. The surface chemistry and acid–base properties of a PAN-based carbon fiber. Carbon 2000;38:675–89.
[22] Weitzsacker CL, Sherwood PMA. X-ray photoelectron spectroscopic studies of carbon fibre surfaces. XIX Surface chemical changes during electrochemical oxidation in base. Surf Int Anal 1995;23:551–8.
[23] Pittman Jr CU, Jiang W, Yue R, Gardner S, Wang L, Toghiani H, et al. Surface properties of electrochemically oxidized carbon fibers. Carbon 1999;37:1797–807.
[24] Waseem SF, Gardner SD, He G, Jiang W, Pittman Jr U. Adhesion and surface analysis of carbon fibres electrochemically oxidized in aqueous potassium nitrate. J Mater Sci 1998;33:3151–62.
[25] Xie Y, Sherwood PMA. Type II pan-based carbon fiber by core level and valence band XPS. Surf Sci Spec 1992;1:216–21.
[26] Vautard F et al. Influence of the carbon fiber surface properties on interfacial adhesion in carbon fiber–acrylate composites cured by electron beam. Compos A-Appl 2011;42:859–67.
[27] Jones C, Sammann E. The effect of low power plasmas on carbon fiber surfaces: a comparison between low and high modulus PAN based fibres with pitch based carbon fibres. Carbon 1990;28:515–9.
[28] Paredes JI, Martínez-Alonso A, Tascón JMD. Oxygen plasma modification of submicron vapor grown carbon fibers as studied by scanning tunneling microscopy. Carbon 2002;40:1101–8.
[29] Okhuysen B, Cochran RC, Allred RE, Spolisi R, Donnellan TM. Interface/interphase studies in epoxy matrix composites. J Adhes 1994;45:3–14.
[30] Li JQ, Huang YD, Fu SY, Yang LH, Qu HT, Wu GS. Study on the surface performance of carbon fibers irradiated by gamma-ray under different irradiation dose. Appl Surf Sci 2010;256:2000–4.
[31] Pino ES, Machado LDB, Glovedi C. Improvement of carbon fiber surface properties using electron beam irradiation. Nucl Sci Technol 2007;18:39–41.
[32] Park SJ, Seo MK, Kim HY, Lee DR. Studies on pan-based carbon fibers irradiated by Ar^+ ion beams. J Colloid Interf Sci 2003;261:393–8.
[33] Fu X, Lu W, Chung DDL. Ozone treatment of carbon fiber for reinforcing cement. Carbon 1998;36:1337–45.
[34] Jin Z, Zhang Z, Meng L. Effects of ozone method treating carbon fibers on mechanical properties of carbon/carbon composites. Mater Chem Phys 2006;97:167–72.
[35] Wilson JIB, Walton JS, Beamson G. Analysis of chemical vapour deposited diamond films by X-ray photoelectron spectroscopy. J Electron Spec 2001;121:183–201.

[36] Jackson ST, Nuzzo RG. Determining hybridation differences for amorphous carbon from the XPS C1s envelope. Appl Surf Sci 1990;90:195–203.
[37] Zielke U, Hüttinger KJ, Hoffman WP. Surface oxidized carbon fibers: II. Chemical modification. Carbon 1996;34:999–1005.
[38] Lakshminarayanan PV, Toghiani H, Pittman Jr CU. Nitric acid oxidation of vapor grown carbon nanofibers. Carbon 2004;42:2433–42.
[39] Alexander MR, Jones FR. Effect of electrolytic oxidation upon the surface chemistry of type a carbon fibres.3. Chemical state, source and location of surface nitrogen. Carbon 1996;34:1093–102.
[40] Schultz J, Nardin M. Determination of the surface energy of solids by the two-liquid-phase method. In: Schrader ME, Loeb G, editors. Modern approaches to wettability: theory and application. New York: Plenum Press; 1992. p. 73–99.
[41] Schultz J, Cazeneuve C, Shanahan MER, Donnet JB. Fibre surface energy characterization. J Adhes 1981;12:221–31.
[42] Gao SL, Mäder E, Zhandarov SF. Carbon fibers and composites with epoxy resins: topography, fractography and interphases. Carbon 2004;42:515–29.
[43] Mason K. Advances in sizings and surface treatment for carbon fibers. High Perform Compos 2004.
[44] Bogoeva-Gaceva G, Mäder E, Häussler L, Share K. Parameters affecting the interface properties in carbon fibre/epoxy systems. Composites 1995;26:103–7.
[45] Wu Z, Pittman Jr CU, Gardner SD. Bonding epoxide functions to nitric acid-oxidized carbon fibers using epichlorohydrin; a reliable analytical determination of epoxide functions on fiber surfaces. Carbon 1995;33:607–16.
[46] Eick JD, Good RJ, Neumann AW. Thermodynamics of contact angles. II. Rough solid surface. J Colloid Interf Sci 1975;53:235–8.
[47] Asloun EM, donnet JB, Guilpain G, Nardin M, Schultz J. On the estimation of the tensile strength of carbon fibers at short lengths. J Mater Sci 1989;24:3504–10.
[48] Drzal LT, Madhukar M. Fiber matrix adhesion and its relationship to composite mechanical properties. J Mater Sci 1993;28:569–610.
[49] Dirand X, Hilaire B, Lafontaine E, Mortaigne B, Nardin M. Crosslinking of vinyl ester matrix in contact with different surfaces. Composites 1994;25:645–52.
[50] Dirand X, Hilaire B, Soulier JP, Nardin M. Interfacial shear strength in glass–fiber/vinylester composites. Compos Sci Technol 1996;56:533–9.
[51] Vautard F. Characterization an optimization of interfaces in composite materials cured by electron beam. PhD Thesis. Haute Alsace University, France; 2006.
[52] Nouranian S, Jang C, Lacy TE, Gwaltney SR, Toghiani H, Pittman Jr CU. Molecular dynamics simulations of vinyl ester resin monomer interactions with a pristine vapour-grown nanofiber and their implications for composite interphase formation. Carbon 2011;49:3219–32.
[53] Allred RE, Hoyt-Haight AE, Gosau JM, Wesson SP. Aqueous-based emulsion reactive finishes for improving carbon/vinyl ester interfacial bonding. In: Proceedings of 50th int. SAMPE symp and exhib. Long Beach, CA, May 1–5, 2005; 2006
[54] Vautard F, Drzal LT. Carbon fiber–vinyl ester interfacial adhesion improvement by the use of a reactive epoxy coating. In: Proceedings of 17th int. conf. on composite materials (ICCM-17). Edinburgh, UK, July 27–31, 2009.
[55] Tsubokawa N. Preparation and properties of polymer-grafted carbon nanotubes and nanofibers. Polym J 2005;37:637–55.

All in-text references underlined in blue are linked to publications on ResearchGate, letting you access and read them immediately.